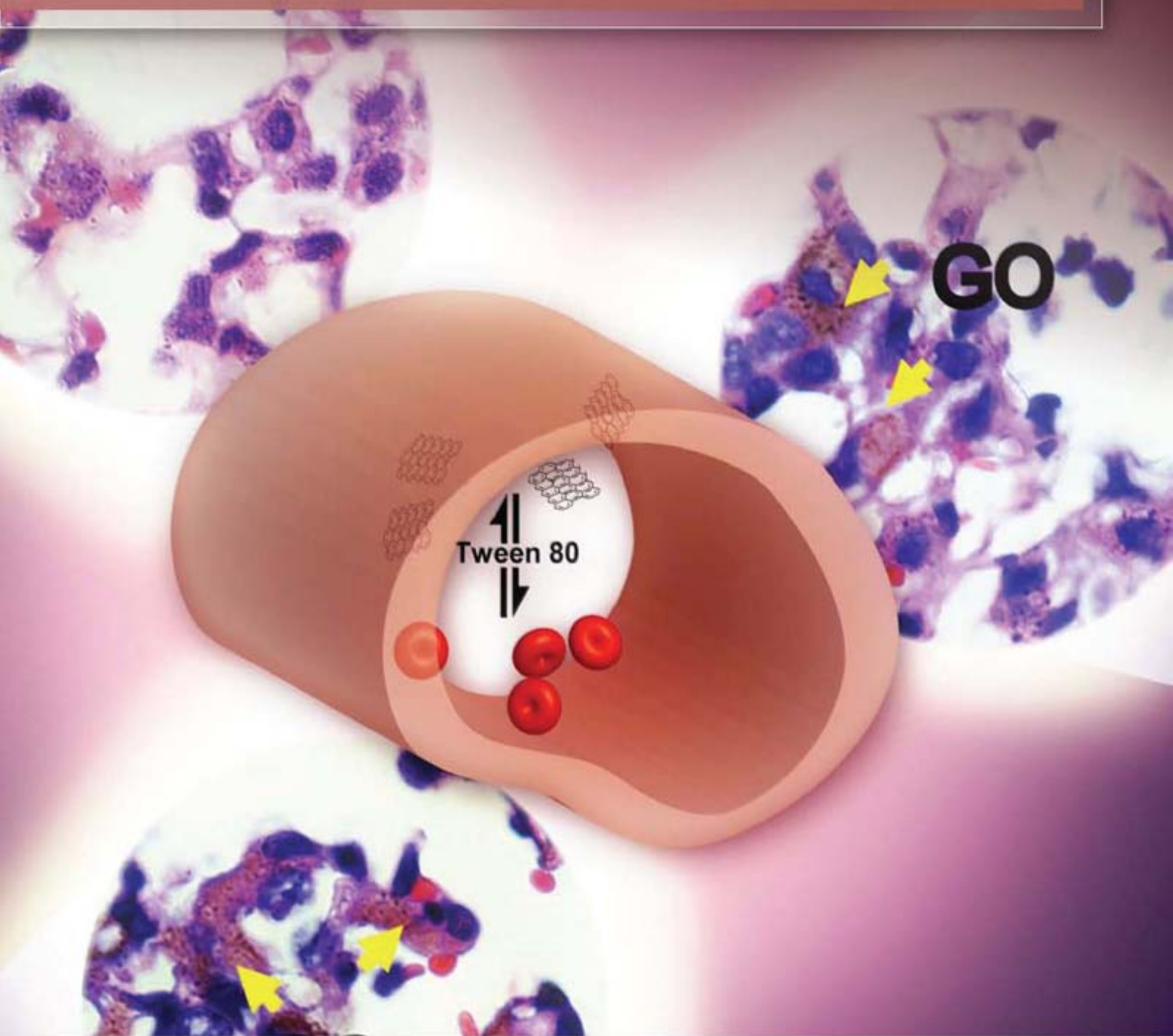


JES

JOURNAL OF
ENVIRONMENTAL
SCIENCES

ISSN 1001-0742
CN 11-2529/X

May 1, 2013 Volume 25 Number 5
www.jesc.ac.cn



Sponsored by
Research Center for Eco-Environmental Sciences
Chinese Academy of Sciences

CONTENTS

Environmental biology

Continuous live cell imaging of cellulose attachment by microbes under anaerobic and thermophilic conditions
using confocal microscopy

Zhi-Wu Wang, Seung-Hwan Lee, James G. Elkins, Yongchao Li, Scott Hamilton-Brehm, Jennifer L. Morrell-Falvey 849

Response of anaerobes to methyl fluoride, 2-bromoethanesulfonate and hydrogen during acetate degradation

Liping Hao, Fan Lü, Lei Li, Liming Shao, Pinjing He 857

Effect of airflow on biodrying of gardening wastes in reactors

F. J. Colomer-Mendoza, L. Herrera-Prats, F. Robles-Martínez, A. Gallardo-Izquierdo, A. B. Piña-Guzmán 865

Environmental health and toxicology

The *ex vivo* and *in vivo* biological performances of graphene oxide and the impact of surfactant on graphene
oxide's biocompatibility (Cover story)

Guangbo Qu, Xiaoyan Wang, Qian Liu, Rui Liu, Nuoya Yin, Juan Ma, Liquan Chen, Jiuyang He, Sijin Liu, Guibin Jiang 873

Determination of the mechanism of photoinduced toxicity of selected metal oxide nanoparticles (ZnO, CuO, Co₃O₄ and
TiO₂) to *E. coli* bacteria

Thabitha P. Dasari¹, Kavitha Pathakoti², Huey-Min Hwang 882

Joint effects of heavy metal binary mixtures on seed germination, root and shoot growth, bacterial bioluminescence,
and gene mutation

In Chul Kong 889

Atmospheric environment

An online monitoring system for atmospheric nitrous acid (HONO) based on stripping coil and ion chromatography

Peng Cheng, Yafang Cheng, Keding Lu, Hang Su, Qiang Yang, Yikan Zou, Yanran Zhao,

Huabing Dong, Limin Zeng, Yuanhang Zhang 895

Formaldehyde concentration and its influencing factors in residential homes after decoration at Hangzhou, China

Min Guo, Xiaoqiang Pei, Feifei Mo, Jianlei Liu, Xueyou Shen 908

Aquatic environment

Flocculating characteristic of activated sludge flocs: Interaction between Al³⁺ and extracellular polymeric substances

Xiaodong Ruan, Lin Li, Junxin Liu 916

Speciation of organic phosphorus in a sediment profile of Lake Taihu II. Molecular species and their depth attenuation

Shiming Ding, Di Xu, Xiuling Bai, Shuchun Yao, Chengxin Fan, Chaosheng Zhang 925

Adsorption of heavy metal ions from aqueous solution by carboxylated cellulose nanocrystals

Xiaolin Yu, Shengrui Tong, Maofa Ge, Lingyan Wu, Junchao Zuo, Changyan Cao, Weiguo Song 933

Synthesis of mesoporous Cu/Mg/Fe layered double hydroxide and its adsorption performance for arsenate in aqueous solutions

Yanwei Guo, Zhiliang Zhu, Yanling Qiu, Jianfu Zhao 944

Advanced regeneration and fixed-bed study of ammonium and potassium removal from anaerobic digested wastewater
by natural zeolite

Xuejun Guo, Larry Zeng, Xin Jin 954

Eutrophication development and its key regulating factors in a water-supply reservoir in North China	
Liping Wang, Lusan Liu, Binghui Zheng	962
Laboratory-scale column study for remediation of TCE-contaminated aquifers using three-section controlled-release potassium permanganate barriers	
Baoling Yuan, Fei Li, Yanmei Chen, Ming-Lai Fu	971
Influence of Chironomid Larvae on oxygen and nitrogen fluxes across the sediment-water interface (Lake Taihu, China)	
Jingge Shang, Lu Zhang, Chengjun Shi, Chengxin Fan	978
Comparison of different phosphate species adsorption by ferric and alum water treatment residuals	
Sijia Gao, Changhui Wang, Yuansheng Pei	986
Removal efficiency of fluoride by novel Mg-Cr-Cl layered double hydroxide by batch process from water	
Sandip Mandal, Swagatika Tripathy, Tapswani Padhi, Manoj Kumar Sahu, Raj Kishore Patel	993
Determining reference conditions for TN, TP, SD and Chl- <i>a</i> in eastern plain ecoregion lakes, China	
Shouliang Huo, Beidou Xi, Jing Su, Fengyu Zan, Qi Chen, Danfeng Ji, Chunzi Ma	1001
Nitrate in shallow groundwater in typical agricultural and forest ecosystems in China, 2004–2010	
Xinyu Zhang, Zhiwei Xu, Xiaomin Sun, Wenyi Dong, Deborah Ballantine	1007
Influential factors of formation kinetics of flocs produced by water treatment coagulants	
Chunde Wu, Lin Wang, Bing Hu, Jian Ye	1015
Environmental catalysis and materials	
Characterization and performance of Pt/SBA-15 for low-temperature SCR of NO by C ₃ H ₆	
Xinyong Liu, Zhi Jiang, Mingxia Chen, Jianwei Shi, Wenfeng Shangguan, Yasutake Teraoka	1023
Photo-catalytic decolourisation of toxic dye with N-doped titania: A case study with Acid Blue 25	
Dhruba Chakraborty, Susmita Sen Gupta	1034
Pb(II) removal from water using Fe-coated bamboo charcoal with the assistance of microwaves	
Zengsheng Zhang, Xuejiang Wang, Yin Wang, Siqing Xia, Ling Chen, Yalei Zhang, Jianfu Zhao	1044
Serial parameter: CN 11-2629/X*1989*m*205*en*P*24*2013-5	



Comparison of different phosphate species adsorption by ferric and alum water treatment residuals

Sijia Gao, Changhui Wang, Yuansheng Pei*

*The Key Laboratory of Water and Sediment Sciences, Ministry of Education, School of Environment,
Beijing Normal University, Beijing 100875, China. E-mail: gaosijia0909@163.com*

Received 21 July 2012; revised 09 October 2012; accepted 17 October 2012

Abstract

As safe byproducts of drinking water treatment processes, ferric and alum water treatment residuals (FARs) have the potential to be new phosphate (P) immobilization materials. In this study, batch experiments were conducted to investigate and compare the adsorption characteristics of three P species by FARs. The results showed that the kinetic processes of different P species' adsorption by FARs could be described by a pseudo second-order model. The ranking list of the initial adsorption rates with respect to different phosphates was pyrophosphate, phytate, orthophosphate, hexametaphosphate and glycerophosphate. Of the six models considered, the two-site Langmuir model most effectively described the adsorption characteristics of the various P species. Upon fitting the results, the maximum adsorption capacities were determined to be 40.24 mg/g for phytate, 18.04 mg/g for pyrophosphate, 17.14 mg/g for orthophosphate, 15.86 mg/g for hexametaphosphate and 10.81 mg/g for glycerophosphate. In addition, the adsorption processes of the different P species were spontaneous endothermic processes and were favored at lower pH values. The pH dependency was found to be especially true for orthophosphate, where the adsorption capacity decreased by 1.22 mg/g with an increase in pH from 5 to 9. Fractionation of the adsorbed P species from the FARs demonstrated that Al-P and Fe-P were the dominating forms, constituting approximately 80%–90% of the total P fractions, which indicated that the adsorbed P species had a low leaching risk and could stably exist in the FARs. Therefore, the FARs could be effective in controlling pollution in water caused by different P species.

Key words: ferric and alum water treatment residuals; different phosphate species; adsorption; phosphate fractions

DOI: 10.1016/S1001-0742(12)60113-2

Introduction

Phosphorous (P) has been regarded as a key element causing eutrophication in surface waters. P in wastewater and surface water exists in various forms such as orthophosphates (ortho-P), condensed phosphates (condensed-P) and organic phosphates (organic-P). Commonly, ortho-P can be utilized by algae directly, whereas condensed-P and organic-P have to undergo hydrolysis in aqueous solution to revert into ortho-P, making them available for immediate biological uptake (Babatunde et al., 2008). Thus, ortho-P are direct contributors to eutrophication, unlike condensed-P and organic-P, which are potential threats.

Ortho-P are usually found in the forms of H_2PO_4^- , HPO_4^{2-} and PO_4^{3-} in water bodies. Condensed-P existing as $\text{P}_2\text{O}_7^{4-}$, $\text{P}_3\text{O}_{10}^{5-}$ and PO_3^- are indispensable assistants of detergents and are also widely used as fertilizers in soil (Dick and Tabatabai, 1987; Guan et al., 2007). Organic-P, such as glycerophosphate and phytate, primary come from

food scraps and human waste. Typically, approximately 25% of total P in settled sewage is present as ortho-P, and 50% of total P in municipal sewage is present as condensed-P and organic-P (Finsten and Hunter, 1967). However, in industrial and agricultural wastewaters, P forms are more complex. In general, the forms and concentrations of P species present in water can be highly varied and particularly source-dependent.

Water treatment residuals (WTRs) are by-products of water treatment plants including four types: Fe-WTRs (only iron salt is used as a coagulant), Al-WTRs (only aluminum salt is used), Fe/Al-WTRs (both ferric and aluminum salt are used, denoted as FARs) and Ca-WTRs (generated from the lime softening process). Studies found WTRs have strong P adsorption capacity owing to their containment of substantial iron and aluminum, which provide a reactive surface and a strong affinity for P (Elliot and Dempsey, 1991; Babatunde and Zhao, 2010; Wang et al., 2011b). The mechanisms of P adsorption onto WTRs involve ligand-exchange, competitive effects with humic

* Corresponding author. E-mail: yspei@bnu.edu.cn

substances and chemical reaction and coprecipitation. Ligand exchange has been demonstrated to be the dominant mechanism for exchanging P with OH^- (Yang et al., 2006; Michael et al., 1998). Many studies have shown that FARs can better adsorb ortho-P (Wang et al., 2011b, 2012; Gao et al., 2012). Less attention has been paid to condensed-P and organic-P, which also have the potential to damage received water. To date, only hexametaphosphate and adenosine monophosphate have been investigated with respect to their adsorption characteristics on Al-WTRs (Razali and Zhao, 2007; Babatunde et al., 2008). The adsorption processes of different P species can be affected by their shapes and sizes as well as their structures. Consequently, it is essential to more deeply understand the characteristics of various P species' adsorption on FARs.

In this study, a contrastive investigation was carried out regarding the adsorption of three P species in five forms by FARs. Kinetic models, isothermal models, thermodynamic study and P fractionation were used to determine the characteristic of each P adsorption on the FARs. The study can provide evidence for the reuse of FARs to control pollution by various P species.

1 Materials and methods

1.1 Materials

FARs were collected from the 9th Water Supply Plant of Beijing, China, where both ferric and aluminum salts are used as coagulants. Samples were air-dried, ground and selected for particles < 80 mesh. The FARs were digested by HNO_3 , HCl and H_2O_2 (US EPA method 3050B), to detect the primary elemental compounds using an Inductively Coupled Plasma-Atomic Emission Spectrometer (ICP-AES, ULTIMA, JY, France). The contents of Fe, Al, Ca and Mg were 89.06, 40.06, 7.10 and 0.64 mg/g, respectively (Fe:Al:Ca:Mg = 125:63:11:1) (Wang et al., 2011b). The surface area of the FARs was measured by the N_2 adsorption-desorption technique using a NOVA-4200e analyzer (USA) and was determined to be 76.83 m^2/g (Wang et al., 2011b).

The ortho-P, condensed-P and organic-P were prepared from sodium dihydrogen phosphate (ortho-P), sodium pyrophosphate (pyro-P) and sodium hexametaphosphate (hexameta-P), sodium glycerophosphate (glycerol-P) and sodium phytate (phytate) (Altundoğan and Tümen, 2003; Li and Guan, 2011; Razali et al., 2007).

Ortho-P was analyzed using the ammonium molybdate spectrophotometric method. The total P was digested to ortho-P using the acid hydrolysis method by heating the samples at 120°C with potassium persulphate salt, then the analysis method was the same as for ortho-P (Du, 2006). The condensed-P and organic-P concentrations were determined by calculating the difference between total P and ortho-P.

1.2 Sorption kinetics

A total of 0.1 g of FARs was loaded into 50-mL polyethylene bottles. Afterward, 20 mL of different P species solutions containing 30 mg-P/L and 0.01 mol/L NaCl were added. The pH value was maintained at 7 by adjusting with NaOH and HCl solutions, and samples were shaken for 2, 4, 8, 12, 16, 24, 36 and 48 hr at 25°C, 120 r/min. Thereafter, the samples were filtered using 0.45- μm Millipore filter paper. Triplicate samples were taken, and the standard error deviation was within 5%.

1.3 Factors affecting P sorption

The different P species solutions containing 30 mg-P/L and 0.01 mol/L NaCl were mixed with the FARs. The ratio of solid to liquid was 1:200 (g/mL). By using 0.1 mol/L HCl or NaOH to adjust the pH, the effect of pH on P sorption was examined at pH 5, 7 and 9. The samples were shaken for 24 hr at 25°C, which was the optimum time determined by the kinetic experiment. Triplicate samples were taken, and the standard error deviation was within 5%.

In a test procedure similar to the above, different initial P concentrations (i.e. 10, 30, 50, 100, 150, 200, 300, 400, 600 mg-P/L) and temperatures (i.e. 288, 298, 308, 318, 328 K) were used to investigate the effects on different P species' adsorption by the FARs. The pH value was maintained at 7 and the shaking time employed was 24 hr.

1.4 P fractionation of the adsorbed P

A mass of 2.5 g of FARs was placed in a 1000-mL Erlenmeyer flask, and 500 mL of a solution with a P concentration of 30 mg/L was then added, followed by shaking for 24 hr at 25°C. The pH was maintained at 7. After adsorption, mixtures were filtered, and the residuals were dried at 50°C.

A sequential P extraction method was implemented for the residuals (Cox et al., 1997; Wang et al., 2011a). The sample was then sequentially extracted with 1 mol/L NH_4Cl (loosely bound P referred to as L-P), 0.5 mol/L NH_4F (Al-P), 0.1 mol/L NaOH (Fe-P), 0.3 mol/L $\text{Na}_3(\text{C}_6\text{H}_5\text{O}_7) \cdot 2\text{H}_2\text{O}$ with 1 g $\text{Na}_2\text{S}_2\text{O}_4 \cdot 2\text{H}_2\text{O}$ (occluded-P referred to as O-P) and 0.5 mol/L H_2SO_4 (Ca-P). The sample was washed twice between each extraction step by suspension in 25 mL of saturated NaCl solution and centrifuged to remove the residual solution of the previous step. The extraction temperature was controlled at 25°C, and the concentrations of ortho-P and total P were determined after each extraction step. Triplicate samples were taken, and the standard error deviation was within 5%.

2 Results and discussion

2.1 Kinetics of different P species adsorption

Figure 1 shows the kinetic curves of different P species' adsorption on FARs. The kinetic curves demonstrated that

the adsorption trends of ortho-P, condensed-P and organic-P by FARs were quite similar. The processes could be modeled in two stages (Sanyal and De Datta, 1991). The first stage was the initial fast adsorption. Owing to a mass of vacant adsorption sites on the FARs surface, P could move rapidly from liquid to the FARs particle exteriors and in macropores (Zumpe et al., 2002; Babatunde and Zhao, 2010). Subsequently, the adsorption capacities of different P species increased significantly. The second stage was the slow equilibrium. The adsorbed P diffused around and inside the FARs surface and precipitated on the surface followed by occlusion. Thus, the adsorption rate decreased. As shown in **Fig. 1**, the adsorption could reach equilibrium in 24 hr, which was determined as an equilibration period for subsequent work.

The pseudo first-order and pseudo second-order equations were applied to describe different P species' adsorption kinetic characteristics by the FARs (**Table 1**). The results showed that the related correlation coefficients (R^2) of the pseudo second-order equation were greater than those of the pseudo first-order equation. Meanwhile, the equilibrium adsorption capacities (q_e) obtained from the former were close to the observed data (q_e'). Therefore, the pseudo second-order equation better described the adsorption processes of different P species, including liquid film diffusion, surface adsorption and intra-particle diffusion

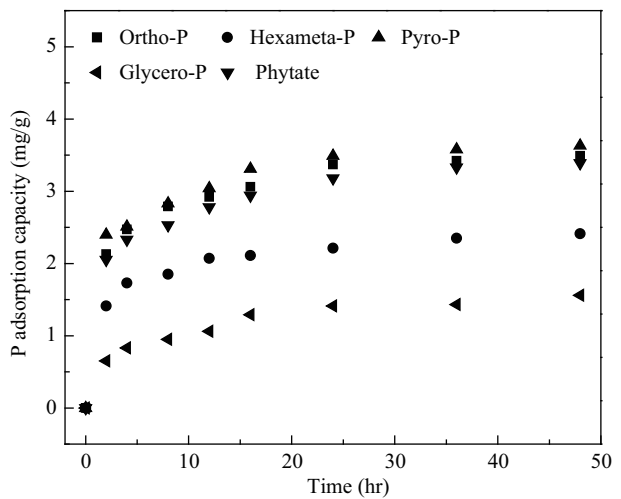


Fig. 1 Kinetics curves of different P species' adsorption on FARs.

(Chang and Juang, 2004). Comparing h values of different P species, the highest initial adsorption rate was obtained for pyro-P (0.043 mg/(g·min)), followed by phytate, ortho-P, hexameta-P and finally glycerol-P. The difference in initial adsorption rate suggested that there were different P structures and different intrinsic affinities between different P and FARs (Guan et al., 2005).

2.2 Effects of initial P concentration

Figure 2 shows the adsorption capacities of FARs for different P species under different initial P concentrations. It could be observed that the adsorption capacities increased with increasing initial P concentrations. The ranking list of the adsorption capacities with respect to different P species for various concentrations was phytate, pyro-P, ortho-P, hexameta-P and glycerol-P. The difference in adsorption capacities could be attributed to the different adsorption mechanisms of ortho-P, condensed-P and organic-P (Razali and Zhao, 2007).

The P adsorption isotherms under different initial concentrations were fitted by the Langmuir, Freundlich, Two-site Langmuir, Temkin, Harkins-Jura and D-R models to determine the sorption characteristics. The parameters of these models are listed in **Table 2**. In view of the R^2 of these models, it could be determined that the highest R^2

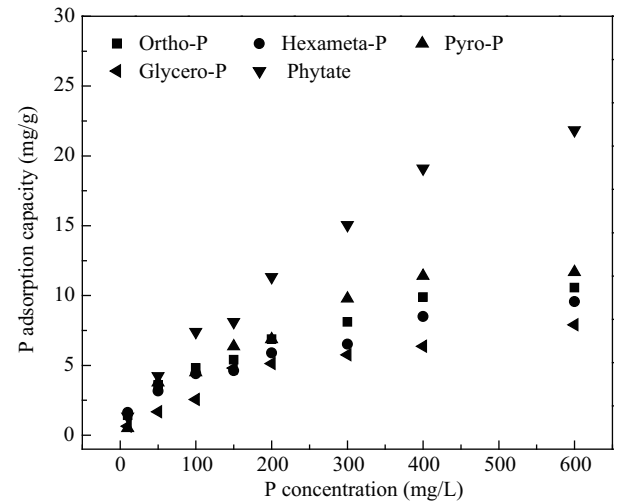


Fig. 2 Adsorption capacities of different P species on FARs under different P concentrations.

Table 1 Parameters for kinetic models of different P species' adsorption on FARs

P species	q_e' (mg/g)	Pseudo first-order kinetic equation			Pseudo second-order kinetic equation			
		$\ln(q_e - q_t) = \ln q_e - K_1 t$			$\frac{t}{q_t} = \frac{1}{K_2 q_e^2} + \frac{t}{q_e}$			
		q_e (mg/g)	K_1 (min ⁻¹)	R^2	q_e (mg/g)	K_2 (g/(mg·min))	h ($K_2 q_e^2$) (mg/(g·min))	R^2
Ortho-P	3.59	3.22	0.006	0.94	3.50	0.003	0.037	0.98
Hexameta-P	2.41	2.17	0.007	0.94	2.38	0.005	0.023	0.99
Pyro-P	3.73	3.31	0.008	0.91	3.60	0.003	0.043	0.97
Glycero-P	1.61	1.42	0.003	0.91	1.63	0.002	0.006	0.96
Phytate	3.46	2.98	0.008	0.93	3.24	0.004	0.039	0.97

q_e' is the actual P adsorption capacity at 48 hr. q_t (mg/g) and q_e are the adsorption capacities at time t and equilibrium, respectively, and K_1 and K_2 are the pseudo first-order and pseudo second-order rate constants, respectively.

was obtained for the Two-site Langmuir, ranging from 0.96 to 0.99, indicating that it was the best model to describe the characteristics of the different P species. The Langmuir, Freundlich, Two-site Langmuir, Temkin, and D-R models also had higher R^2 values ranging 0.75 to 0.99, except for that of pyro-P for D-R ($R^2 = 0.68$). However, the poor fit of the Harkins-Jura model resulted in lower R^2 values (0.65–0.84).

The parameters K and n reflected the adsorption capacity and adsorption strength of the FARs, respectively. As listed in **Table 2**, the K and n values for the different P species varied. FARs presented the best adsorption strength for ortho-P, followed by condensed-P and organic-P, which may be attributed to the different shapes and sizes of the various P molecules.

Comparing the fitting results of the Langmuir and Two-site Langmuir models, it could be observed that the latter fitted the data better. Therefore, q_m of the Two-site Langmuir model has usually been used to estimate the theoretical maximum P adsorption capacity (Wang et al., 2011a). The Two-site Langmuir model is a modification of the classical Langmuir isotherm model assuming that the sorption occurs either on two types of surfaces, each with different bonding energies, or on one surface with two distinct energies (Bolster and Hornberger, 2007). A more complex model would probably include too many adjustable parameters to allow a realistic interpretation of their values (Angovel et al., 1998). Therefore, the Two-site Langmuir isotherm model can describe the data closely, and the fitted parameters give a consistent description of the characteristics of different P species' adsorption on FARs. q_{m1} and q_{m2} represented the P adsorption capacity

at two types of surfaces, respectively, and the maximum P adsorption capacity was the sum of q_{m1} and q_{m2} . Ranking the list of the maximum P adsorption capacities with respect to different P species yields phytate (44.24 mg/g), pyro-P (18.05 mg/g), ortho-P (17.14 mg/g), hexameta-P (15.86 mg/g) and glycerol-P (10.81 mg/g). This result indicated that the P absorption capacity largely depended on the P molecular structure (Guan et al., 2005). For example, the four functional groups of the phytate molecule were attached to the aluminum hydroxide surface and formed four nuclear complexes when phytate was adsorbed. However, the structure of the complexes formed between ortho-P/condensed-P and metal hydroxide surface were monodentate, bidentate, or binuclear (Ognalaga et al., 1994). Therefore, each P functional group of phytate occupied a smaller area compared with other phosphates; thus, more phytate could be adsorbed than other species (Celi et al., 1999, 2001).

2.3 Effects of pH

The effects of pH on different P species' adsorption are shown in **Fig. 3**. The adsorption capacities of ortho-P, condensed-P and organic-P on FARs were highly influenced by pH; in particular, low pH values were favorable for P adsorption. Correspondingly, the adsorption capacities decreased with increasing pH. The largest adsorption capacity occurred at a pH of 5 in this study, and the removal rates of different P species by the FARs ranged from 28.63% to 64.74%. As the pH of the solution was raised from 5 to 9, the adsorption capacities of ortho-P, hexameta-P, pyro-P, glycerol-P and phytate decreased by 1.22, 0.54, 0.73, 0.58 and 0.66 mg/g, respectively. The

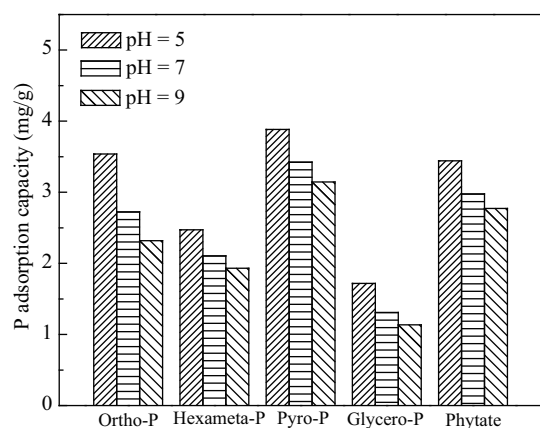
Table 2 Fitting results of the adsorption isotherm experiment of FARs (pH = 7)

Models	Equation	Parameters	Ortho-P	Hexameta-P	Pyro-P	Glycero-P	Phytate
Freundlich	$q_e = KC_e^{\frac{1}{n}}$	K (L/mg)	0.59	0.52	0.54	0.37	0.38
		n	2.28	2.19	2.13	1.85	1.56
		R^2	0.98	0.98	0.96	0.96	0.99
Langmuir	$q_e = \frac{q_m b C_e}{1 + b C_e}$	b (L/mg)	0.0053	0.0051	0.0037	0.0041	0.0020
		q_m (mg/g)	13.91	12.19	17.24	11.34	41.65
		R^2	0.97	0.92	0.97	0.95	0.98
Two-site Langmuir	$q_e = q_{m1} \frac{b_1 C_e}{1 + b_1 C_e} + q_{m2} \frac{b_2 C_e}{1 + b_2 C_e}$	q_{m1} (mg/g)	2.15	2.59	1.00	4.91	0.78
		b_1	0.13	0.14	0.04	0.004	1.09
		q_{m2} (mg/g)	14.99	13.27	17.05	5.89	43.46
		b_2	0.002	0.001	0.003	0.004	0.002
		R^2	0.99	0.99	0.96	0.97	0.99
		R^2	0.92	0.88	0.92	0.90	0.85
Temkin	$q_e = B_1 \ln(K_T C_e)$	B_1	2.26	1.86	2.87	1.79	4.99
		K_T (L/mg)	0.13	0.15	0.08	0.09	0.07
		R^2	0.92	0.88	0.92	0.90	0.85
Harkins-Jura	$\frac{1}{q_e} = \frac{B}{A} - \frac{1}{A} \log C_e$	A	3.98	5.19	0.52	0.80	12.21
		B	2.47	2.54	2.39	2.43	8.29
		R^2	0.76	0.84	0.65	0.75	0.72
D-R	$q_e = q_m e^{-K \varepsilon^2}$	q_m (mg/g)	8.81	7.52	11.28	7.03	20.46
		K (mol ² /kJ ²)	0.0007	0.0006	0.0017	0.0015	0.0013
		E (kJ/mol)	26.73	28.88	17.14	18.26	19.61
		R^2	0.75	0.68	0.83	0.90	0.86

q_m , q_{m1} and q_{m2} are the maximum P adsorption capacities; C_e (mg/L) is the equilibrium P concentration.

Table 3 Thermodynamic and adsorption parameters at different temperatures

P species	ΔH^0 (kJ/mol)	ΔS^0 (J/(mol·K))	ΔG^0 (kJ/mol)				
			288 K	298 K	308 K	318 K	328 K
Ortho-P	37.94	171.78	−11.53	−13.25	−14.97	−16.69	−18.40
Hexameta-P	31.95	145.35	−9.91	−11.36	−12.82	−14.47	−11.29
Pyro-P	53.70	224.66	−10.99	−13.25	−15.49	−17.74	−19.99
Glycerol-P	24.43	115.96	−8.97	−10.12	−11.29	−12.45	−13.61
Phytate	31.83	150.33	−11.47	−12.97	−14.47	−15.98	−17.48

**Fig. 3** Effectiveness of P species' adsorption on FARs at various pH values.

various decreases could be related to either the P structures or functional groups (Altundoğan and Tümen, 2001). According to Yang et al. (2006), P was mainly adsorbed by ligand exchange between P and OH^- . An increase in pH would lead to a rise in OH^- ions, which would occupy more active sites on the surfaces of FARs and enhance the competitive strength with P. Meanwhile, the increasing amount of OH^- ions would induce the formation of a new charged counter-ion layer, which would reject P adsorption (Ye et al., 2006). Apart from these factors, the pH at the point of zero charge (pH_{PZC}) also played an important role in the adsorption processes (Hamdi and Srasra, 2012). The pH_{PZC} of FARs was approximately 7.5 (Yang et al., 2006), and the surface charge of FARs would be positive at a pH less than the pH_{PZC} . Consequently, at lower pHs, P adsorption would be facilitated by electrostatic and chemical attraction onto the abundantly positive charged surface. However, as pH rose above the pH_{PZC} , the surface charge of FARs became predominantly negative and P adsorption decreased.

2.4 Effects of temperature

The distribution coefficient (K_d , mL/g), the standard free energy (ΔG^0 , kJ/mol), the standard enthalpy (ΔH^0 , kJ/mol), and the standard entropy (ΔS^0 , J/(mol·K)) were used to confirm the processes of different P species' adsorption at different temperatures (Kilislioglu et al., 2003). They were calculated by the following equations:

$$K_d = \frac{C_0 - C_e}{C_e} \times \frac{V}{m} \quad (1)$$

$$\ln K_d = -\frac{\Delta H^0}{RT} + \frac{\Delta S^0}{R} \quad (2)$$

$$\Delta G^0 = \Delta H^0 - T\Delta S^0 \quad (3)$$

The adsorption capacities of different P species at various temperature values are illustrated in **Fig. 4a**. The ΔH^0 and ΔS^0 values were determined by the slopes and intercepts of linear regression of $\ln K_d$ vs. $1/T$ (**Fig. 4b**). The values of ΔH^0 , ΔS^0 and ΔG^0 are shown in **Table 3**. As shown in **Fig. 4**, the adsorption capacities and K_d of all P species increased with increasing temperature, indicating the endothermic nature of adsorption (Kilislioglu and Bilgin., 2003). Increasing the temperature is known to increase the rate of diffusion of the adsorbate molecules across the external boundary layer and in the internal pores of the adsorbent particle, owing to the decrease in the viscosity of the solution (Al-qodah, 2000). The ΔH^0 values were positive for ortho-P, hexameta-P, pyro-P, glycerol-P and phytate (ranging from 24.43 to 53.70 kJ/mol), which indicated that the adsorption reactions of the different P species on FARs were endothermic. The ΔS^0 values for all P species were greater than zero, which could be the result of water molecules previously bonded to the metal ions being released and dispersed in the solution when P was adsorbed onto the FARs surface (Oguz, 2005). The ΔG^0 values for all the systems were negative ($-8.97 < \Delta G^0 < -19.99$) and decreased with increasing temperature, indicating that the different P species' adsorption reactions were spontaneous processes.

2.5 Fractionation of the adsorbed P

The results of P fractionation are presented in **Fig. 5**. The amount of total extracted P as ortho-P, hexameta-P, pyro-P, glycerol-P and phytate was 3.44, 2.24, 3.55, 1.52 and 3.31 mg/g, respectively, which accounted for 95.84%, 93.19%, 95.52%, 94.12% and 95.79% of the adsorbed P, respectively. The results indicated that the adsorbed P could stably exist in FARs and had a low leaching risk. Meanwhile, ortho-P, condensed-P and organic-P adsorbed on the FARs mainly existed in the forms of Al-P and Fe-P, which accounted for approximately 80%–90% of total P, while only small percentages were determined to be L-P, O-P and Ca-P. Fractions of ortho-P decreased in the following order: Al-P (52.62%), Fe-P (31.71%), O-P (5.81%), L-P (3.64%) and Ca-P (1.89%). For condensed-P

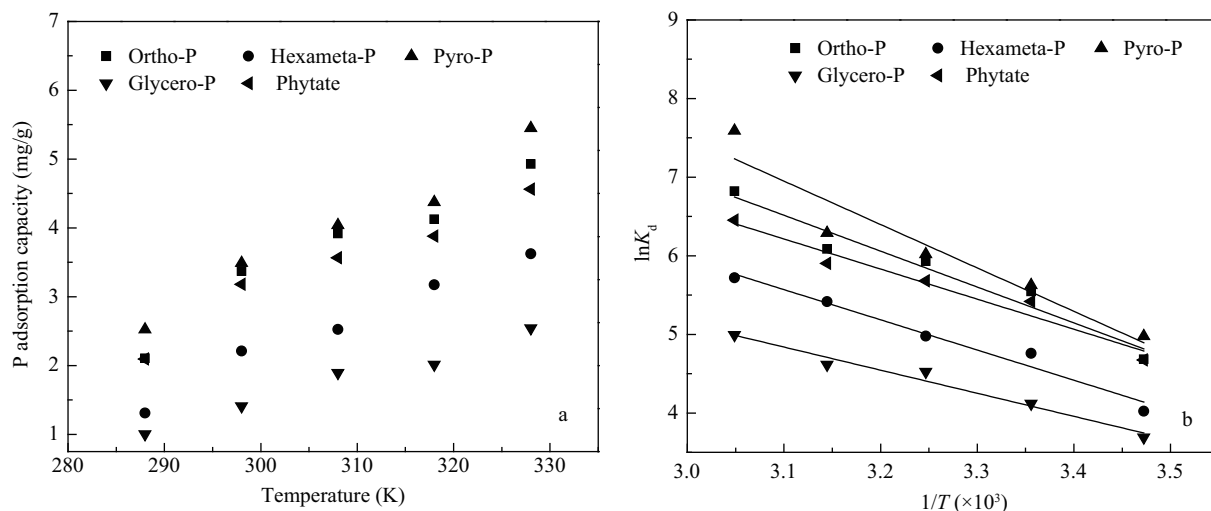


Fig. 4 (a) Effect of temperature on different P species' adsorption by FARs; (b) plot of $\ln K_d$ vs. $1/T$ for different P species.

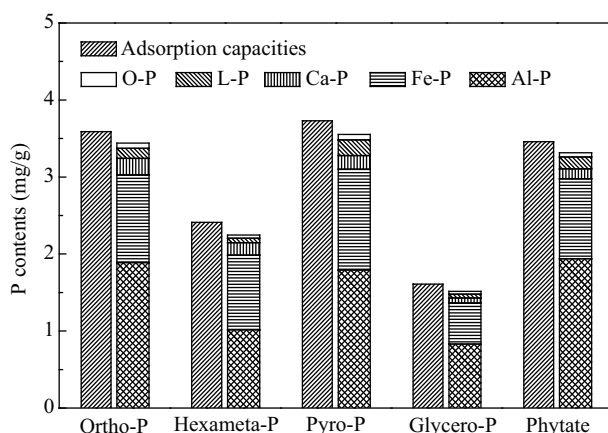


Fig. 5 Fractionation of absorbed P in FARs.

and organic-P, similar orders of different P fractions were observed.

In Dayton's research, it was demonstrated that amorphous Fe and Al had been considered to be favorable for P adsorption (Dayton and Basta, 2005). The contents of Fe and Al in the FARs were 89.06 mg/g and 40.06 mg/g, respectively, and were found in relatively higher concentrations than other elements (Wang et al., 2011b). Fe and Al had a high affinity for P sorption due to positive Fe-P and Al-P precipitation. In addition, because of their high charge density, Al^{3+} and Fe^{3+} may strongly attach the anion of P to FARs (Gan et al., 2009). Therefore, the combination of Fe and Al mainly contributed to the adsorption of ortho-P, condensed-P and organic-P on FARs.

3 Conclusions

The FARs had strong adsorption abilities for ortho-P, condensed-P and organic-P. The adsorption processes of different P species were similar, and could be roughly divided into the fast adsorption and slow equilibrium stages, and were well described by the pseudo second-

order equation. The initial adsorption rate of each P species was considerably different, and the observed maximum rate was for pyrophosphate (0.043 mg/(g·min)) while the observed minimum rate was for glycerophosphate (0.006 mg/(g·min)). The adsorption capacities fitted by the Two-site Langmuir isotherms varied for the different P species as well as with the pH of the P suspension. The ranking list of highest adsorption capacity with respect to different phosphates was determined to be phytate, pyro-P, ortho-P, hexameta-P and finally glycerol-P. P adsorption favored acidic suspensions rather than alkaline suspensions for all three types of P species tested. Moreover, the adsorption reactions of different P species were spontaneous endothermic processes. In addition, the adsorbed P on FARs mainly existed in the forms of Al-P and Fe-P and hardly desorbed from FARs. These findings could be significant for the efficient reuse of FARs as low-cost P adsorption materials.

Acknowledgments

This research was supported by the National Natural Science Foundation of China (No. 51278055, 51179008).

References

- Al-qodah Z, 2000. Adsorption of dyes using shale oil ash. *Water Research*, 34(17): 4295–4303.
- Altundoğan H S, Tümen F, 2001. Removal of phosphates from aqueous solutions by using bauxite I: Effect of pH on the adsorption of various phosphates. *Journal of Chemical Technology and Biotechnology*, 77(1): 77–85.
- Altundoğan H S, Tümen F, 2003. Removal of phosphates from aqueous solutions by using bauxite II: the activation study. *Journal of Chemical Technology and Biotechnology*, 78(7): 824–833.
- Angove M J, Johnson B B, Wells J D, 1998. The influence of temperature on the adsorption of cadmium(II) and cobalt (II) on kaolinite. *Journal of Colloid and Interface Science*, 204(1): 93–103.
- Babatunde A O, Zhao Y Q, Yang Y, Kearney P, 2008. Reuse of

- dewatered aluminum-coagulated water treatment residual to immobilize phosphorus: Batch and column trials using a condensed phosphate. *Chemical Engineering Journal*, 136(2-3): 108–115.
- Babatunde A O, Zhao Y Q, 2010. Equilibrium and kinetic analysis of phosphorus adsorption from aqueous solution using waste alum sludge. *Journal of Hazardous Materials*, 184(1-3): 746–752.
- Bolster C H, Hornberger G M, 2007. On the use of linearized Langmuir equations. *Soil Science Society of America Journal*, 71(6): 1796–1806.
- Celi L, Lamacchia S, Marsan F A, Barberis E, 1999. Interaction of inositol hexaphosphate on clays: adsorption and charging phenomena. *Soil Science*, 164(8): 574–585.
- Celi L, Presta M, Ajmore-Marsan F, Barberis E, 2001. Effects of pH and electrolytes on inositol hexaphosphate interaction with goethite. *Soil Science Society of America Journal*, 65(3): 753–760.
- Chang M Y, Juang R S, 2004. Adsorption of tannic acid, humic acid, and dyes from water using the composite of chitosan and activated clay. *Journal of Colloid and Interface Science*, 278(1): 18–25.
- Cox A E, Camberato J J, Smith B R, 1997. Phosphate availability and inorganic transformation in an alum sludge-affected soil. *Journal of Environmental Quality*, 26(5): 1393–1398.
- Dayton E A, Basta N T, 2005. A method for determining the phosphorus sorption capacity and amorphous aluminum of aluminum-based drinking water treatment residuals. *Journal of Environmental Quality*, 34(3): 1112–1118.
- Dick R P, Tabatabai M A, 1987. Polyphosphates as sources of phosphorus for plants. *Fertilizer Research*, 12(2): 107–118.
- Du S, 2006. *Soil Analysis Specification* (2nd ed.). China Agricultural Press, Beijing, China. 52.
- Elliot H A, Dempsey B A, 1991. Agronomic effects of land application of water treatment sludges. *Journal American Water Works Association*, 84(4): 126–131.
- Finstein M S, Hunter J V, 1967. Hydrolysis of condensed phosphates during aerobic biological sewage treatment. *Water Research*, 1(4): 247–254.
- Gan F Q, Zhou J M, Wang H Y, Du C W, Chen X Q, 2009. Removal of phosphate from aqueous solution by thermally treated natural palygorskite. *Water Research*, 43(11): 2907–2915.
- Gao S J, Wang C H, Pei Y S, 2012. Effects of phosphate removal by thermal- and acid-activated ferric and alum water treatment residuals. *Acta Scientiae Circumstantiae*, 32(3): 606–611.
- Guan X H, Chen G H, Shang C, 2005. Competitive adsorption between orthophosphate and other phosphates on aluminum hydroxide. *Soil Science*, 170(5): 340–349.
- Guan X H, Chen G H, Shang C, 2007. Adsorption behavior of condensed phosphate on aluminum hydroxide. *Journal of Environmental Sciences*, 19(3): 312–318.
- Hamdi N, Srasra E, 2012. Removal of phosphate ions from aqueous solution using Tunisian clays minerals and synthetic zeolite. *Journal of Environmental Sciences*, 24(4): 617–623.
- Kilislioglu A, Bilgin B, 2003. Thermodynamic and kinetic investigations of uranium adsorption on amberlite IR-118H resin. *Applied Radiation and Isotopes*, 58(2): 155–160.
- Li C, Guan X H, 2011. Competitive adsorption of three different phosphate species on aluminum hydroxide. *Fresenius Environmental Bulletin*, 20(8): 1936–1941.
- Michael A B, Domenico G, Cristian P S, Hotze W, 1998. Surface complexation modeling of phosphate adsorption by water treatment residual. *Journal of Environmental Quality*, 27(5): 1055–1063.
- Ognalaga M, Frossard E, Thomas F, 1994. Glucose-1-phosphate and myo-inositol hexaphosphate adsorption mechanisms on goethite. *Soil Science Society of America Journal*, 58(2): 332–337.
- Oguz E, 2005. Thermodynamic and kinetic investigations of PO_4^{3-} adsorption on blast furnace slag. *Journal of Colloid and Interface Science*, 281(1): 62–67.
- Razali M, Zhao Y Q, Bruen M, 2007. Effectiveness of a drinking-water treatment sludge in removing different phosphorus species from aqueous solution. *Separation and Purification Technology*, 55(3): 300–306.
- Sanyal S K, De Datta S K, 1991. Chemistry of phosphorus transformations in soils. *Advances in Soil Science*, 16: 1–120.
- Wang C H, Gao S J, Wang T X, Tian B H, Pei Y S, 2011a. Effectiveness of sequential thermal and acid activation on phosphorus removal by ferric and alum water treatment residuals. *Chemical Engineering Journal*, 172(2-3): 885–891.
- Wang C H, Guo W, Tian B H, Pei Y S, Zhang K J, 2011b. Characteristics and kinetics of phosphate adsorption on dewatered ferric-alum residuals. *Journal of Environmental Science and Health Part A*, 46(14): 1632–1639.
- Wang C H, Wang Z Y, Lin L, Tian B H, Pei Y S, 2012. Effect of low molecular weight organic acids on phosphorus adsorption by ferric-alum water treatment residuals. *Journal of Hazardous Materials*, 203-204: 145–150.
- Yang Y, Zhao Y Q, Babatunde A O, Wang L, Ren Y X, Han Y, 2006. Characteristics and mechanisms of phosphate adsorption on dewatered alum sludge. *Separation and Purification Technology*, 51(2): 193–200.
- Ye H P, Chen F Z, Sheng Y Q, Sheng Y G, Fu J M, 2006. Adsorption of phosphate from aqueous solution onto modified palygorskites. *Separation and Purification Technology*, 50(3): 283–290.
- Zumpe H, Baskaran K, Dharmabalan P, 2002. Reuse of Water Treatment Plant Sludge for Phosphorus Removal (3rd ed.). World Water Congress, Melbourne, Australia.

JOURNAL OF ENVIRONMENTAL SCIENCES

环境科学学报(英文版)
(<http://www.jesc.ac.cn>)

Aims and scope

Journal of Environmental Sciences is an international academic journal supervised by Research Center for Eco-Environmental Sciences, Chinese Academy of Sciences. The journal publishes original, peer-reviewed innovative research and valuable findings in environmental sciences. The types of articles published are research article, critical review, rapid communications, and special issues.

The scope of the journal embraces the treatment processes for natural groundwater, municipal, agricultural and industrial water and wastewaters; physical and chemical methods for limitation of pollutants emission into the atmospheric environment; chemical and biological and phytoremediation of contaminated soil; fate and transport of pollutants in environments; toxicological effects of terrorist chemical release on the natural environment and human health; development of environmental catalysts and materials.

For subscription to electronic edition

Elsevier is responsible for subscription of the journal. Please subscribe to the journal via <http://www.elsevier.com/locate/jes>.

For subscription to print edition

China: Please contact the customer service, Science Press, 16 Donghuangchenggen North Street, Beijing 100717, China. Tel: +86-10-64017032; E-mail: journal@mail.sciencep.com, or the local post office throughout China (domestic postcode: 2-580).

Outside China: Please order the journal from the Elsevier Customer Service Department at the Regional Sales Office nearest you.

Submission declaration

Submission of an article implies that the work described has not been published previously (except in the form of an abstract or as part of a published lecture or academic thesis), that it is not under consideration for publication elsewhere. The submission should be approved by all authors and tacitly or explicitly by the responsible authorities where the work was carried out. If the manuscript accepted, it will not be published elsewhere in the same form, in English or in any other language, including electronically without the written consent of the copyright-holder.

Submission declaration

Submission of the work described has not been published previously (except in the form of an abstract or as part of a published lecture or academic thesis), that it is not under consideration for publication elsewhere. The publication should be approved by all authors and tacitly or explicitly by the responsible authorities where the work was carried out. If the manuscript accepted, it will not be published elsewhere in the same form, in English or in any other language, including electronically without the written consent of the copyright-holder.

Editorial

Authors should submit manuscript online at <http://www.jesc.ac.cn>. In case of queries, please contact editorial office, Tel: +86-10-62920553, E-mail: jesc@263.net, jesc@rcees.ac.cn. Instruction to authors is available at <http://www.jesc.ac.cn>.

Journal of Environmental Sciences (Established in 1989)

Vol. 25 No. 5 2013

Supervised by	Chinese Academy of Sciences	Published by	Science Press, Beijing, China
Sponsored by	Research Center for Eco-Environmental Sciences, Chinese Academy of Sciences		Elsevier Limited, The Netherlands
Edited by	Editorial Office of Journal of Environmental Sciences P. O. Box 2871, Beijing 100085, China Tel: 86-10-62920553; http://www.jesc.ac.cn E-mail: jesc@263.net , jesc@rcees.ac.cn	Distributed by	
		Domestic	Science Press, 16 Donghuangchenggen North Street, Beijing 100717, China Local Post Offices through China
		Foreign	Elsevier Limited http://www.elsevier.com/locate/jes
Editor-in-chief	Hongxiao Tang	Printed by	Beijing Beilin Printing House, 100083, China
CN 11-2629/X	Domestic postcode: 2-580	Domestic price per issue	RMB ¥ 110.00

ISSN 1001-0742

